Transition
Innovative resilient farming systems in Mediterranean environments

Deliverable 2.3

Report on EO detection of agroforestry systems (horizontal intensification and spatio-temporal diversity)

PRIMA programme is supported by Horizon 2020, the European Union's Framework Programme for Research and innovation.

PRIMA
PARTNERSHIP FOR RESEARCH AND INNOVATION IN THE MEDITERRANEAN AREA

Transition
Innovative resilient farming systems in Mediterranean environments

Document history

Date (YYYY/MM/DD)	Author (Name Surname)	Action	Status
2023.05.23	Dimitrios Vallianatos Themistoklis Herekakis	1st draft	Draft
2023.05.31	Themistoklis Herekakis	2nd draft	Final

PRIMA programme is supported by Horizon 2020, the European Union's Framework Programme for Research and innovation.

PRIMA PARTNERSHIP FOR RESEARCH AND INNOVATION IN THE MEDITERRANEAN AREA

TABLE OF CONTENTS

List of Tables

List of Figures

List of Boxes

List of Abbreviations

EO	Earth Observation
NDVI	Normalized Difference Vegetation Index
Rao Q	Rao's Quadratic entropy index

PRIMA programme is supported by Horizon 2020, the European Union's Framework Programme for Research and innovation.

DESCRIPTION

This is the report document for Deliverable 2.3 "Report on EO detection of agroforestry systems" of the TRANSITION project and relates to the use of Earth Observation (EO) methods for detecting innovative agricultural systems for regional, national, and EU authorities necessary for policy guidance, monitoring, and inspections.

The structure of Deliverable 2.3 report is as follows:

- Chapter 1 describes the main objective and sub-objectives of the project with a focus on the need for detection methods to map agricultural areas in the Mediterranean region.
- Chapter 2 describes the methodological approach, including data collection, and mapping the horizontal intensification and spatio-temporal diversity.
- Chapter 3 presents the results of the deliverable.
- Chapter 4 presents the conclusions of the report.

The data acquired and produced during the implementation of this task and deliverable are available in the attached DATA folder. In addition, a data repository will be created within the project, where the produced results – including this deliverable – will be stored. The list of generated data is as follows:

- MODIS NDVI datasets: 46 image tiff files of NDVI for each demonstration area for the year 2022.
- GlobCorine data: Global landcover data acquired from Bontemps et al. (2009).
- Horizontal agricultural intensification products: 4 spatial raster files (.tiff) files of the results produced through K-means clustering.
- Spatio-temporal diversity products: 5 spatial raster files (.tiff) of the results produced from the estimation of Rao Q.

1. INTRODUCTION

The Mediterranean region has a unique climate characterized by mild, wet winters and hot, dry summers. Sustainable agriculture in this region is currently facing a significant challenge, primarily due to climate change as it has directly impacted rainfall patterns, leading to changes in the frequency of rain events, floods, and droughts. These changes, in turn, affect the productivity of land and water resources as well as the livelihoods of farmers. The region is also experiencing increasing land use change pressures due to urban expansion and economic and infrastructural development. The existing cultivated land is under pressure from multiple sources, including growing food demand from an increasing population, climate change effects, land degradation, water scarcity, and rural abandonment. As, future projections suggest a substantial decrease in agricultural production in the Mediterranean region, , it is crucial to implement rational agricultural land use planning to address future food requirements and effectively manage available land resources in a sustainable manner.

1.1. EO detection methods for agricultural applications in the Mediterranean region

New strategies and decision-making processes are urgently required to ensure the sustainable utilization of environmental resources and address the current and future challenges faced by global agricultural systems. Developing detection and monitoring methods based on EO in the Mediterranean region is crucial for effective agricultural management and planning, adaptation to climate change, water resource management, land use planning, and early warning systems, all of which are important components to efficiently address local and regional challenges. The advancements in technology, such as earth observation (EO), (digital) geospatial technologies, unmanned aerial vehicles (UAVs), and the Internet of Things (IoT), have revolutionized our understanding of agricultural systems and their intricate interactions at ecological, social, and economic levels. EO technologies can efficiently serve land use mapping and monitoring , identification of areas suitable for agriculture and consequently support land use planning decisions. By gaining an additional lens and better understand the dynamics of land-use, policymakers and land managers can make informed choices regarding agricultural expansion, conservation of natural areas, and the balance of various land use demands. Using EO it data on land cover, vegetation health, crop growth, and other relevant parameters are collected timely and objectively at regional level. Such information is

vital for monitoring the condition of agricultural areas, identifying potential issues or risks, and implementing timely management strategies.

The goal of TRANSITION is to pave the way for a transition towards resilient agriculture in the Mediterranean, maximizing the net positive impact on the environment, while increasing the resilience of agroecosystems, rural societies, and return on assets to farmers. This will be achieved by: 1) identifying appropriate strategies for adoption to improve the resilience of the agriculture sector, including using locally-adapted genetic resources, unconventional water reuse, and soil protection strategies; 2) establishing what are the environmental and socio-economic barriers to resilient agriculture implementation; 3) quantifying the system productivity and delivery of ecosystem services of existing systems and co-designed and replicable case studies and their effect on farmers' livelihoods; 4) empowering the expansion of agroforestry and mixed farming systems through practical innovation and knowledge exchange and; 5) providing robust information which is useful to administrations in terms of measurable impacts and possible transition scenarios which maximize ecological services delivery and resilience of key Mediterranean cropping systems. The current document constitutes Deliverable 2.3, which contributes towards providing a resilient farming system implementation roadmap to increase the sustainability of farming systems and livelihood protection on the basis of systematically collected knowledge on the existing systems on a regional level.

1.2. The context of the deliverable within the TRANSITION project and the related work packages

Task 2.3 aims, more specifically, at the detection of ecologically-intensified agricultural systems with Earth Observation (EO). The technical focus of this task will be in using courser resolution satellite datasets (MODIS) to analyze agricultural activities over a growing season. The mandate is to identify horizontal (agriculture area expansion) and spatio-temporal diversity (linked to the number of crops cultivated in space and time, fallow land, one-two crops, etc.) of agricultural use during a specific timeframe. For a more detailed explanation see the following sections 2.2, 2.3, 3,1, and 3.2.

The produced workflow can be applied to detect agricultural systems and extract important information that local regional, national, and EU level authorities and policymakers can use for policy guidance, monitoring, and inspections ensuring an efficient and sustainable management of agricultural ecosystems.

2. METHODOLOGY

2.1. Satellite data

The Normalized Difference Vegetation Index (NDVI) is one of the most successful attempts to simply and quickly identify vegetated areas and their "condition". It remains the most well-known and used index to detect live green plant canopies in multispectral remote sensing data. Chlorophyll strongly absorbs visible light, and the cellular structure of the leaves strongly reflects near-infrared light. When the plant becomes dehydrated, sick, afflicted with disease, etc., the spongy layer deteriorates, and the plant absorbs more of the near-infrared light, rather than reflecting it. Thus, by using NDVI and by observing how NIR changes compared to red light provides an accurate indication of the presence of chlorophyll, which correlates with plant health. As shown below, Normalized Difference Vegetation Index (NDVI) uses the NIR and red channels in its formula with healthy vegetation (chlorophyll) reflecting more near-infrared (NIR) and green light compared to other wavelengths.

$$NDVI = \frac{(NIR - Red)}{(NIR + Red)}$$

These spectral reflectances, are themselves ratios of the reflected radiation to the incoming radiation in each spectral band individually, hence they take on values between 0 and 1; therefore, NDVI ranges between -1 and +1. Negative values are mainly formed from clouds, water and snow, and values close to zero are primarily formed from rocks and bare soil. Very small values (0.1 or less) of the NDVI function correspond to empty areas of rocks, sand or snow. Moderate values (from 0.2 to 0.3) represent shrubs and meadows, while large values (from 0.6 to 0.8) indicate temperate and tropical forests.

The widely used MODIS vegetation indices provide consistent spatial and temporal information and allow analysing terrestrial vegetation conditions across large areas (Solano et al., 2010). Following the rationale of Estel et al. (2015), we used the MODIS NDVI time series of sixteen-day composites from the satellites Terra (MOD13Q1, v5) and Aqua (MYD13Q1, v5) from 01-01-2022 to 31-12-2022 at a spatial resolution of approximately 250 m. The MODIS NDVI time series were downloaded using the R package "*MODIStsp*" (Busetto & Ranghetti, 2016) and the function "*MODIStsp*". Code example of the downloading process in given in Box 1. The code scripts used for each

demonstration are shown in Annex 1. Note that the methodology and R script demonstrated in this deliverable can be easily replicated for other or multiple years.

Box 1. Example code snippet for downloading MODIS EVI and NDVI times series (source: https://docs.ropensci.org/MODIStsp/articles/noninteractive_execution.html).

```
install.packages("remotes")
library(remotes)
install_github("ropensci/MODIStsp")
library(MODIStsp)

# **NOTE** Output files of examples are saved to file.path by setting out_folder to
$tempdir.

# --> See name and available layers for product M*D13Q1
# MODIStsp_get_prodlayers("M*D13A2")

# --> Launch the processing
MODIStsp(
  gui             = FALSE,
  out_folder      = "$tempdir",
  selprod         = "Vegetation_Indexes_16Days_1Km (M*D13A2)",
  bandsel         = c("EVI", "NDVI"),
  quality_bandsel = "QA_usef",
  indexes_bandsel = "SR",
  user            = "mstp_test" ,
  password        = "MSTP_test_01",
  start_date      = "2020.06.01",
  end_date        = "2020.06.15",
  verbose         = FALSE,
  parallel        = FALSE
)

# Outputs are in this case in subfolder "MODIStsp/VI_16Days_1Km_v6" of
# `base::tempdir()`:

out_fold <- file.path(tempdir(), "MODIStsp/VI_16Days_1Km_v6/")
list.files(out_fold)
list.files(file.path(out_fold ,"EVI"))
list.files(file.path(out_fold ,"QA_usef"))
```

The NDVI time series of Aqua (MYD13Q1) and Terra (MOD13Q1) were combined to improve the quality of the time series by increasing the usable observations within the studied year 2022. Combining both Aqua and Terra time series resulted in 46 image composites for 2022 for each demonstration area. All downloaded products are listed in Annex 2.

To define the extent of potentially active or fallow farmland (i.e. all cropland and grassland) for the study area, we used the GlobCORINE land-cover map (Bontempset al., 2009), derived via a regionally-tuned classification of seasonal and annual mosaics of ENVISAT's Medium Resolution Imaging Spectrometer (MERIS) from December 2004 to June 2006 at a spatial resolution of 300 m (Figure 1). GlobCORINE has an overall

accuracy of ~ 90% (Defourny et al., 2010) and adapts, to the extent possible, an aggregated CORINE class catalog.

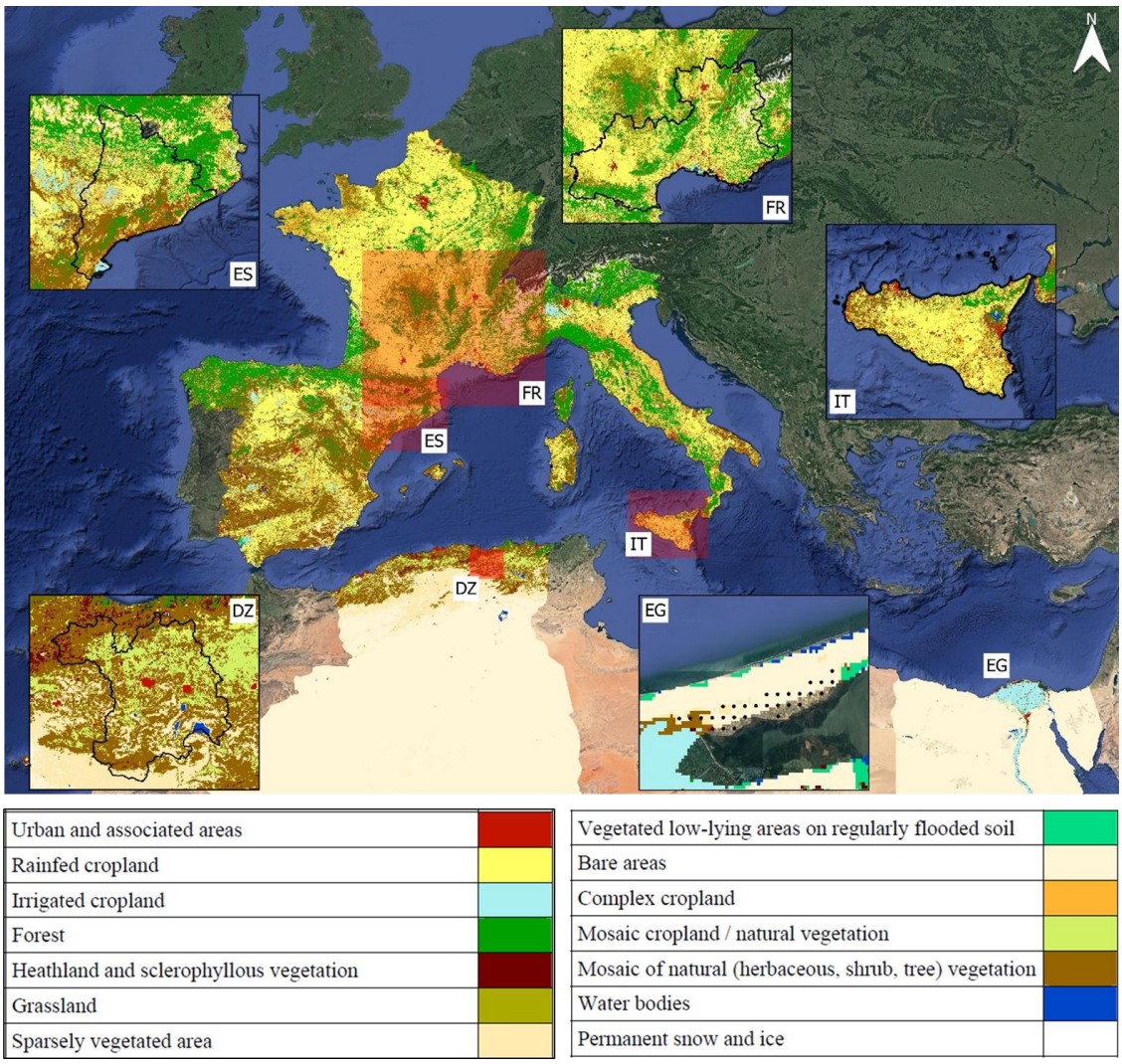

Figure 1. GlobCORINE data acquired for the countries to which the demonstration areas are located (Spain-ES, France-FR, Italy-IT, Algeria-DZ and Egypt-EG).

We generated a mask that excluded forests, urban areas, barren land, and ice, and focused our analyses on the GlobCORINE classes rainfed cropland, irrigated cropland, grassland, complex cropland (annual crops associated with permanent crops and complex cultivation patterns), mosaic of cropland/natural vegetation, and mosaic of natural vegetation (herbaceous, shrub, tree). We included the grassland and natural vegetation mosaic classes in our mask to cover unmanaged areas and that could represent fallow areas recultivated at a later period (Figure 2). The main crops for each case study area are described in Table 1.

Table 1. Case study areas and their main crops.

Case study country	Main crop(s)
Algeria, Satif	Cereal (durum wheat, barley, and oats), potatoes
Egypt	Cereals, rice, vegetables
France, Marseille	grapes. olives, orchards, vegetables: cereals and others
Italy, Sicily	Citrus, wine grapes, olives, tomatoes, nuts.
Spain, Catalonia	Cereals (wheat, barley, maize), olives, grapes, citrus fruits, and vegetables

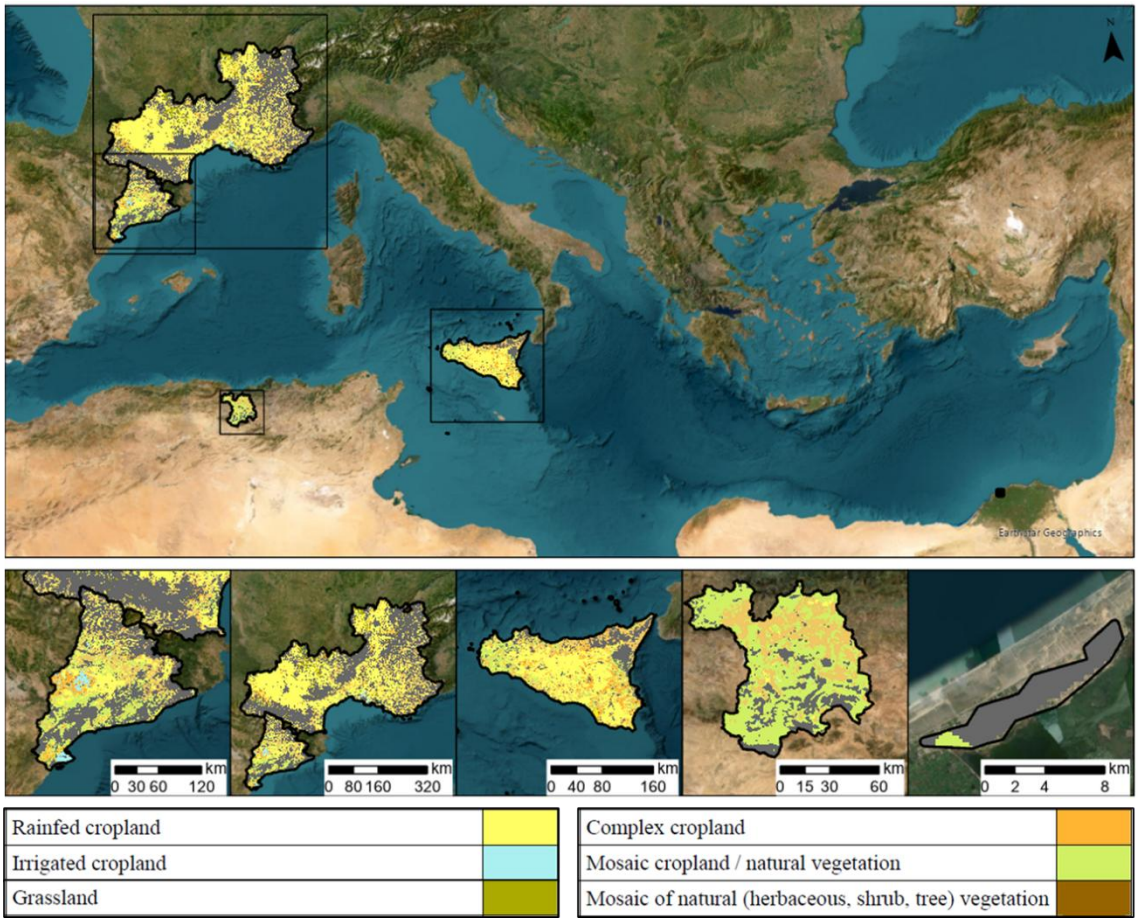

Figure 2. Masked areas representing croplands, grasslands, and cropland/natural vegetation categories; grey areas indicate areas excluded from the analysis (urban areas, forests, water bodies etc.).

2.2. Mapping horizontal intensification of agricultural use

To detect horizontal intensification of agricultural use, we followed a step-by-step procedure: 1) we extracted NDVI values for agricultural regions only; 2) we created NDVI

time-series plots to reveal the temporal variations of NDVI throughout the year, and; 3) selected the most appropriate NDVI image to map agriculture area expansion.

To extract NDVI values for areas representing agricultural areas we used the mask created in the previous section. For each image in the time-series we estimated mean NDVI values to showcase intra-annual variability in NDVI values. By visualising and inspecting the MODIS time series data plots, we identified the most appropriate date base the detection of agricultural area expansion on (Figure 3).

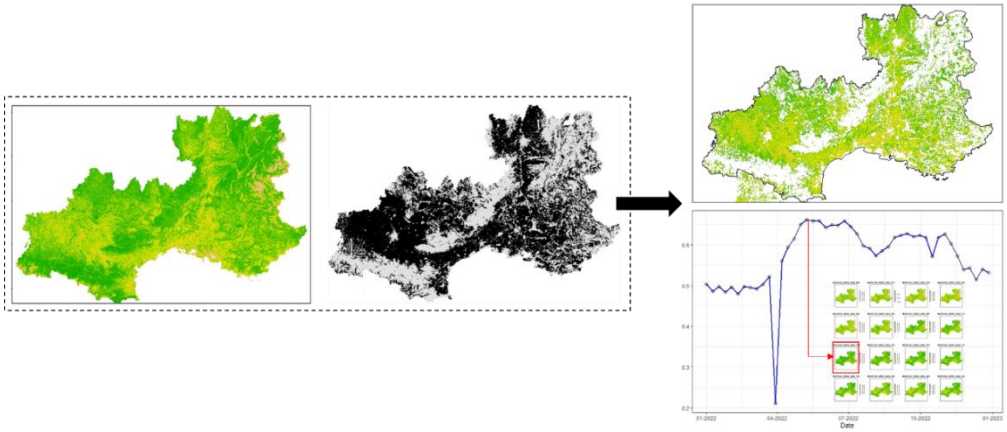

Figure 3. Workflow for selecting the most appropriate date to map the expansion of agricultural areas using coarse resolution MODIS satellite images.

This above process was applied to all demonstration areas except for the Egyptian case study as its small size would not allow a “confident” interpretation of the results. In addition, based on the GlobCorine data, the majority of the Egyptian demonstration area is not considered as cropland leading to only a few observations (raster cells) being included in the analysis.

As shown in Figure 4, the mean NDVI value is characterized by irregular temporal profiles with both positive and negative peaks being evident throughout the year. Assuming that in the agricultural region positive peaks indicate the peak of the growing season, we selected an image within the spring-summer period where NDVI showed the highest positive peaks. However, in the case of the Sicily in Italy, as the highest NDVI peak values were observed during the winter period we chose a peak between the summer and autumn season as an indication of possible harvesting period.

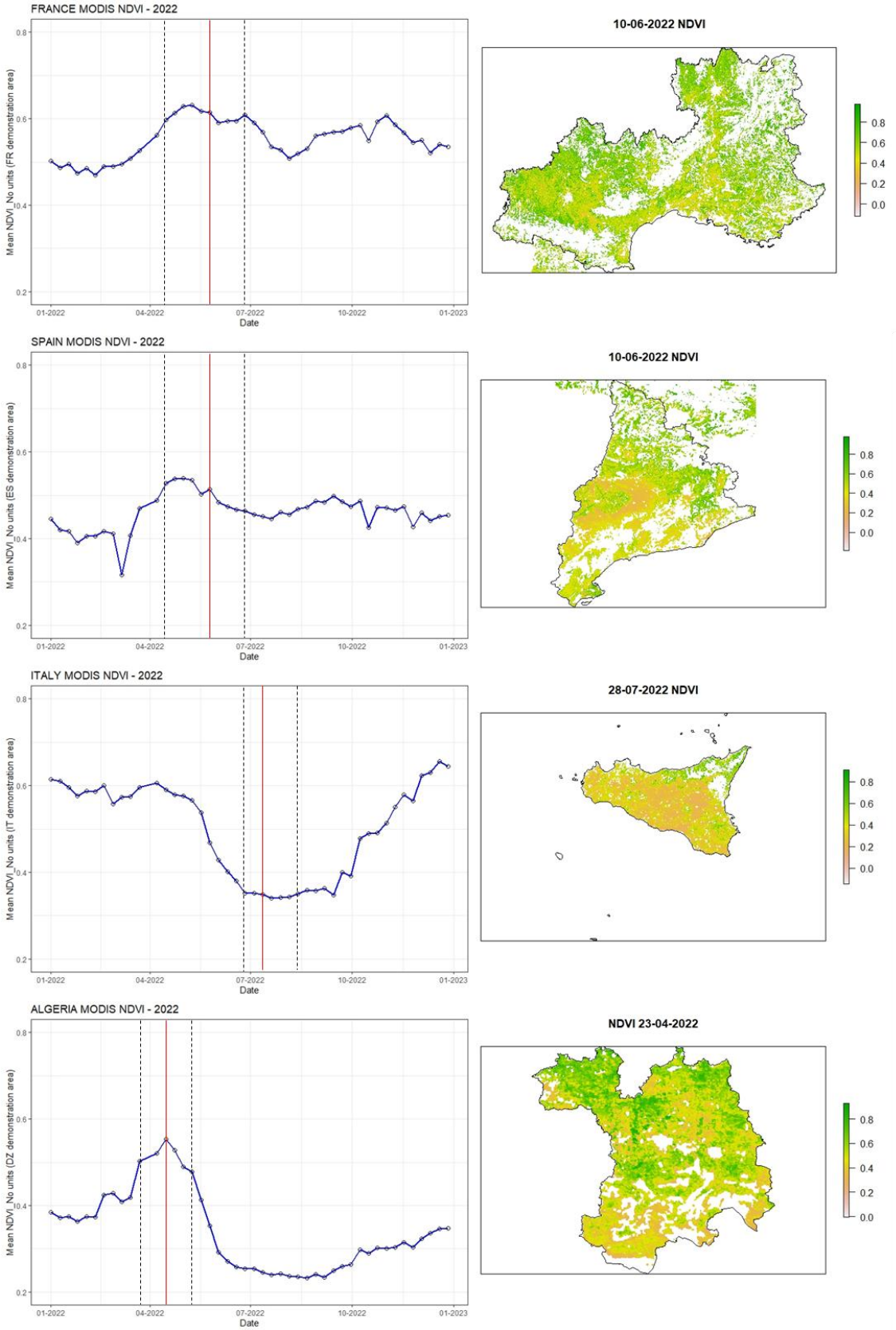

Figure 4. Left: Time series of the Mean MODIS NDVI value across agricultural areas of the demonstration areas; Right: NDVI for the selected year used for the k means clustering classification.

Following the selection of the most appropriate NDVI for the four demonstration areas, we applied a K-means clustering algorithm to segregate the image pixels into clusters based on their related spectral characteristics. The K-means algorithm attempts to find sets of cluster centres that describe the distribution of the points in the dataset by minimising the sum of the squared distances between each point and its cluster centre. For a given number of clusters (K), it first assigns the cluster centres by randomly selecting K points from the dataset (Golubovic et al., 2019). It then alternates between assigning points to the cluster represented by the nearest centre, and recomputing the centres, while decreasing the overall sum of squared distances (Lloyd, 1982; Bishop & Nasrabadi, 2006).

2.3. Mapping spatio-temporal diversity of agricultural use

To map the spatio-temporal diversity of agricultural use (e.g. number or diversity of crops) within a region, we employed the open-source method developed by Rocchini et al., 2017; 2019) for measuring diversity changes through remote sensing. Their work was based on the application of Rao's Quadratic entropy index to remotely sensed data, providing a straightforward R function to calculate it in 2D systems. The script and function developed by Rocchini et al. to derive Rao's Q, is written in the R statistical language (R Core Team, 2023), and is stored in the GitHub repository https://github.com/mattmar/spectralrao.

Understanding agricultural vertical changes in time is crucial to promptly inform management practices against diversity loss. However, agricultural management and planning is mainly based on field observations related to crop diversity, considering different crop species, under the assumption of robust statistical sampling and proper methods of analysis. Such a method is time and cost consuming and does not allow in most cases to get temporal replicates. Rao's Q is computed as the sum of all the pixel values pairwise distances, each of which is multiplied by the relative abundance of each pair of pixels in the analyzed image. In other words, Rao's Q is the expected difference (distance) in reflectance values under the hypothesis of random allocation of pixels. In our case, we interpret Rao's Quadratic entropy as an index of spatio-temporal agro-ecosystem diversity. We highlight the methodology’s links to spatial complexity or landscape and crops (Nguyen et al. 2022), and temporal intensification (Tsardanidis et

al. 2025) of farming, i.e., number of crops, crop destruction practices (e.g., mowing, destruction), tillage events, and others.

The MODIS NDVI time-series data downloaded for the horizontal agricultural intensification are also used for detecting the vertical intensification. An example of Rao Q index applied in NDVI data is shown below (Figure 5).

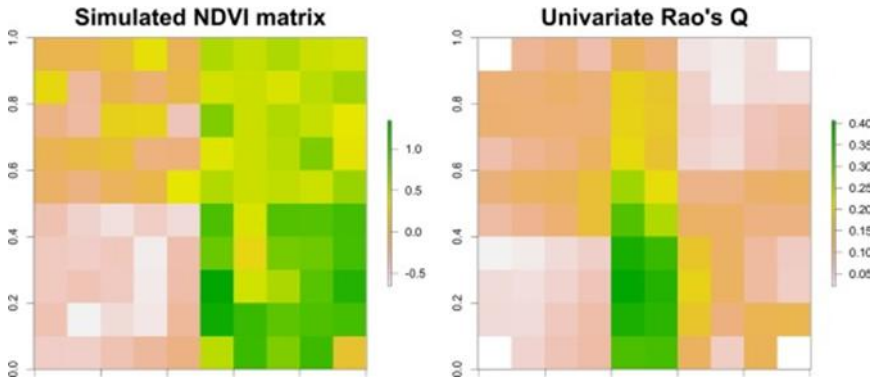

Figure 5. An example of the calculation of Rao Q index on a simulated NDVI image.

The image above demonstrates how Rao Q takes into account neighbouring pixels to estimate the diversity among pixels. If one focuses on the bottom and middle part of the two images it is clear that the difference between low and high NDVI values (left image) results in high values of the Rao Q index. While at the bottom left of the NDVI image where mostly low values of NDVI are evident, this dominance (of low NDVI values) resulted in low Rao Q diversity. For the purposes of this deliverable, we applied the above methodology taking into account both the spectral diversity within a single image as well as the multidimensionality of the time-series data. Therefore, to estimate the vertical intensification of agriculture we used the NDVI images representing the peak values as demonstrated in the previous section Figure 4. The periods which we take into consideration when estimating Rao Q for each country is given in Table 2.

Table 2. Months for which the MODIS NDVI images were used for the estimation of Rao Q index.

Demonstration areas of:	**Period (months) considered**
France	April - July
Spain	April - July
Italy	July - August
Algeria	March - May
Egypt	March - April

3. RESULTS AND DISCUSSION

3.1. Horizontal intensification of agricultural use

Results from the detection of the horizontal intensification of agricultural use showed a similar distribution pattern compared to the Global Corine data. Specifically, the detection maps based on MODIS exhibited similar clustering groups with the categories found in Global Corine. In the case of the European demonstration areas in France, Spain, and Italy (Sicily), the “Rainfed cropland” is also evident in the MODIS-based maps (Figures 6 and 7) we produced. For the Algerian demonstration area, the “Complex cropland” and “Mosaic cropland / natural vegetation” classes seem to also follow a similar pattern in both the Global Corine and MODIS maps (Figure 7). However, the “Grassland” and “Complex cropland” classes showed that a clear distinction between the two could not be achieved in some areas. This was the case for Sicily where these two classes appeared as one in the results of the MODIS workflow.

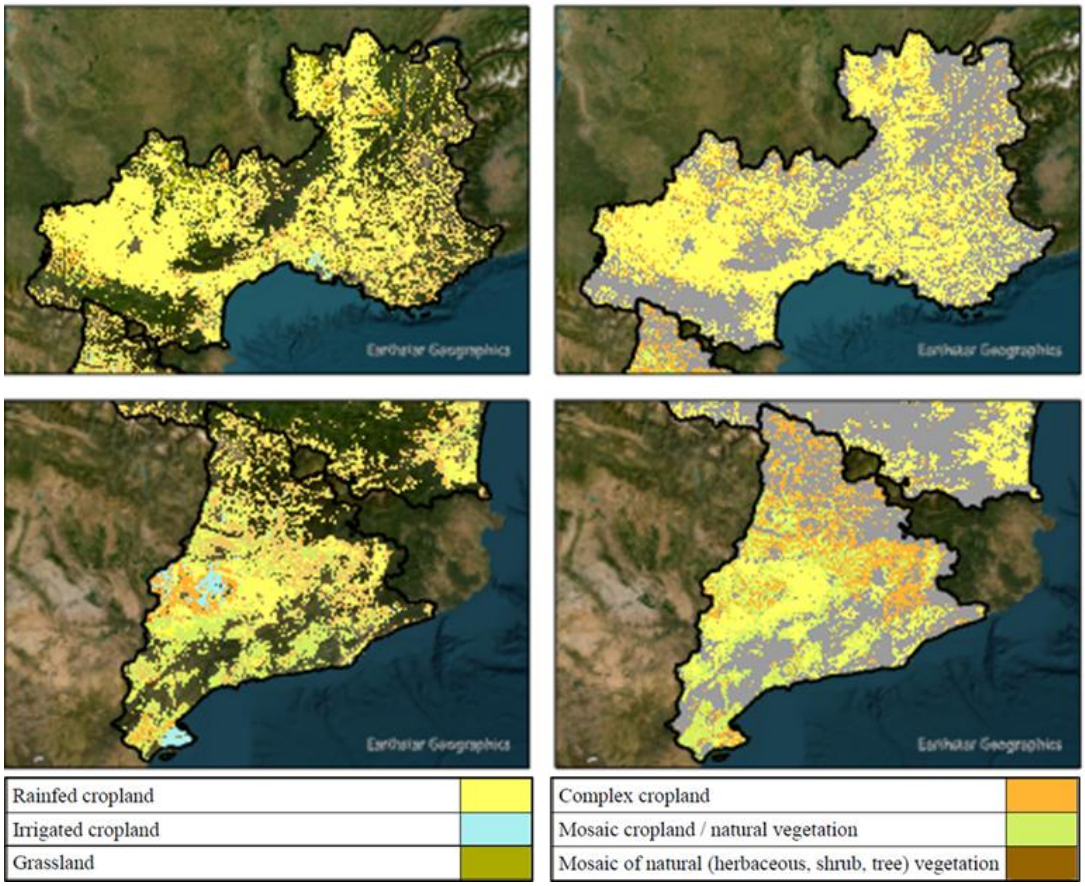

Figure 6. Results from the detection of the horizontal intensification of agricultural use in the French and Spanish demonstrations areas (Left: Global Corine agricultural land cover; Right: Agricultural area expansion as detected using K-means clustering); Grey areas indicate urban areas and water bodies.

In general, the applied methodology demonstrated that by using coarser resolution satellite images such as MODIS it was possible to identify the patterns of not only the agricultural area expansion but also the patterns of specific agricultural/crop categories.

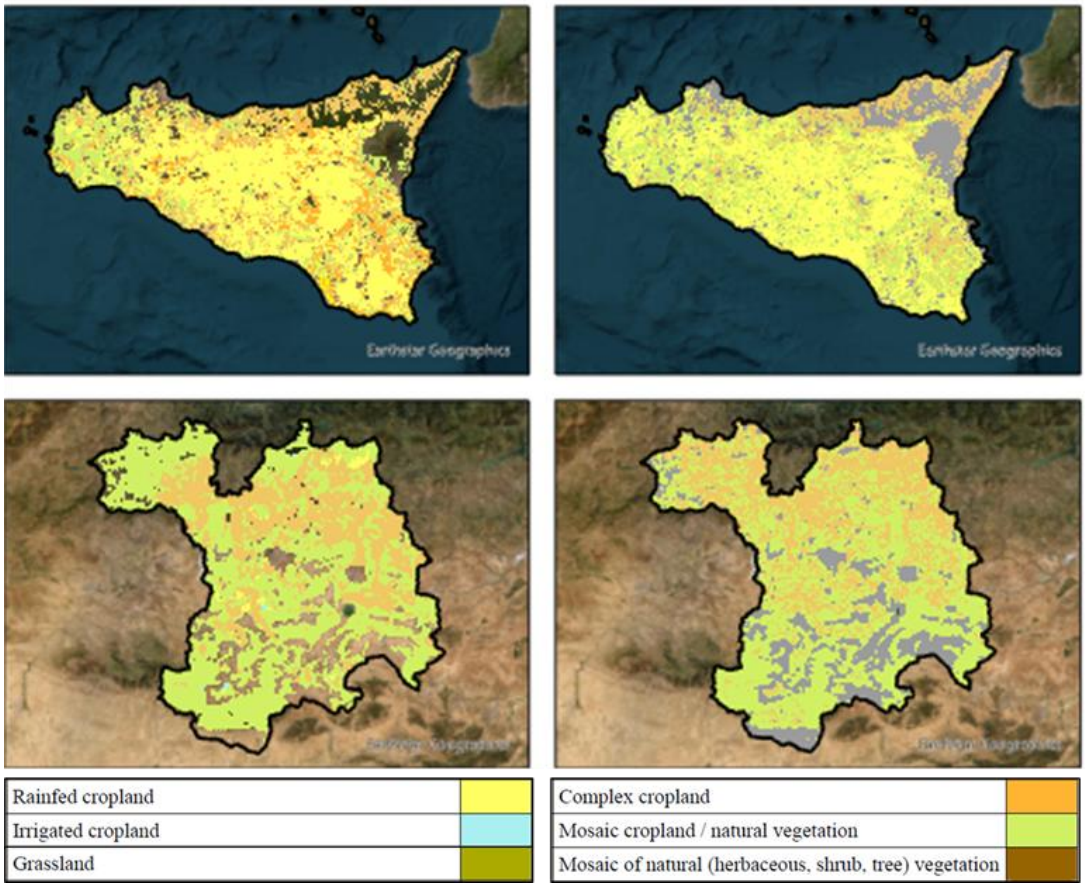

Figure 7. Results from the detection of the horizontal intensification of agricultural use in the Italian and Algerian demonstrations areas (Left: Global Corine agricultural land cover; Right: Agricultural area expansion as detected using K-means clustering); Grey areas indicate urban areas and water bodies.

3.2. Spatio-temporal diversity of agricultural use

Results from the detection of spatio-temporal diversity showed different patterns among all demonstration areas (Figure 8). Regions with higher values of Rao Q can exhibit spatial diversity of crops, i.e., multiple crops within a given area, as well as temporal diversity, i.e., changed spectral profile of crops within a given period. This suggests that crop that crops have been harvested within the assessed period, that within the assessed period, the initial (planting) and crop development (flowering) stage occurred, some kind of management practice has occurred (e.g., mowing, destruction), or more rarely that categories might have changed through time. The inverse holds for low values of Rao Q (single crop areal and temporal dominance, limited use of mowing or other destructive practices, no harvest, or that there is similar spectral information of that of neighboring areas (or pixels).

In the French demonstration areas, central regions are dominated mainly by rainfed croplands (e.g., maize, soybean, sunflower) that exhibited low temporal diversity, indicating that such crops remained, for the most part, the same between April – July. However, in the west region where rainfed crops are also dominant, higher values of Rao Q diversity were observed indicating either spatial or temporal diversity of crops. Spatial diversity of crops seems to be the case for most regions in the Spanish demonstration area, as in regions were two or multiple cropland categories are evident higher values of Rao Q were observed. In Sicily, complex cropland and grasslands appear as areas with high diversity crops. Similar to the French case study, rainfed croplands in the Spanish region and Sicily exhibited lower diversity values. In the case of Setif in Algeria, the mosaic of cropland and natural vegetation as well as the complex croplands that characterize the central region led to higher observations of Rao Q. Although, the southern part of the croplands in Setif are dominated by a mosaic of crops and natural vegetation, areas in that region seem to exhibit lower temporal diversity values. Finally, to avoid possibly inaccurate interpretation for the Egyptian demonstration area due to its considerably small size and coarse resolution of MODIS data, we avoided any explanation regarding the detection of vertical agricultural use.

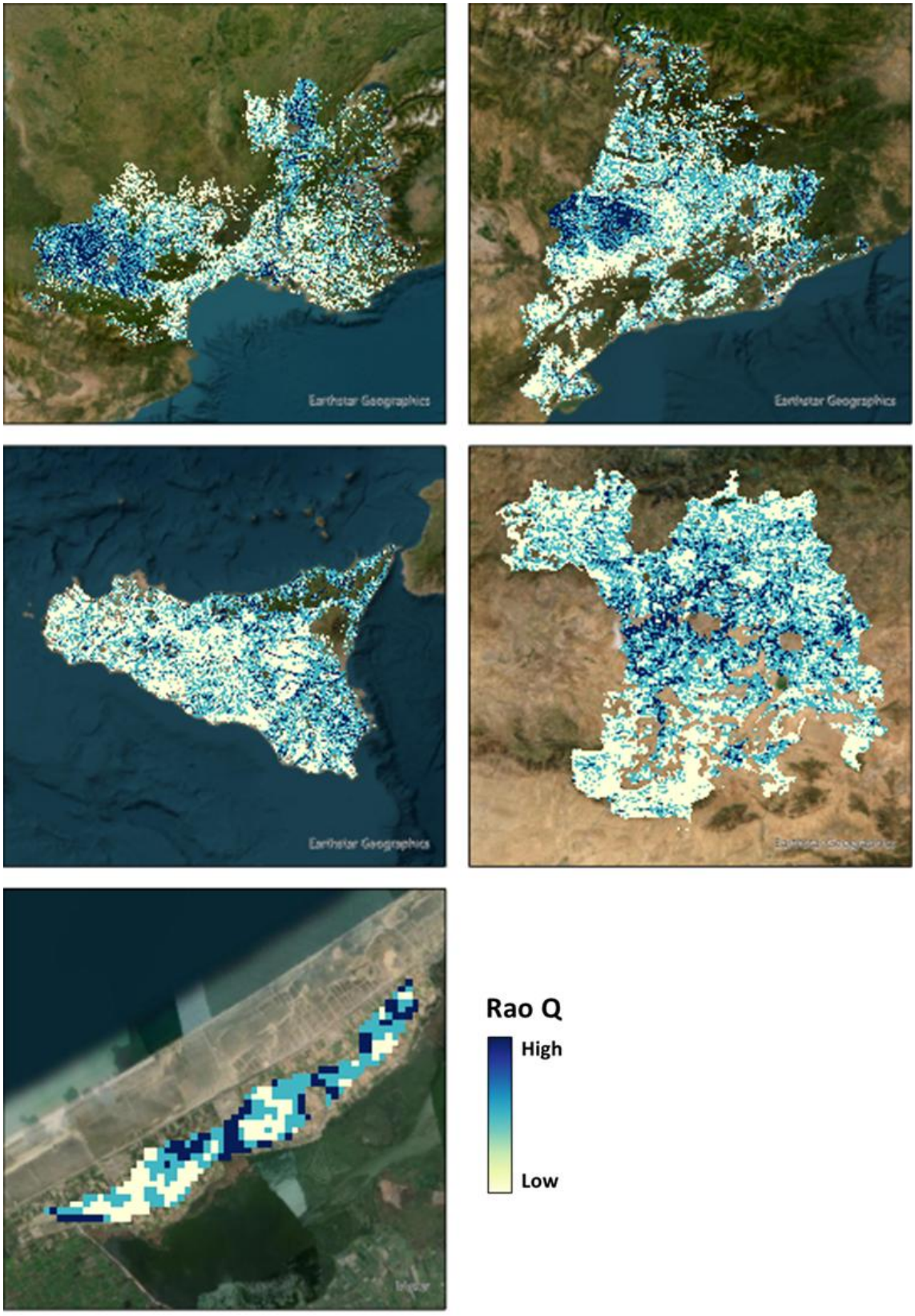

Figure 8. Results from the detection of the vertical intensification of agricultural use across the demonstrations areas.

4. CONCLUSIONS

In this report, we present a robust workflow to estimate horizontal intensification and spatio-temporal diversity use across TRANSITION'S demonstration areas. Furthermore, since we include here the code for analysis and the necessary data are freely accessible (MODIS satellite images), we expect high reproducibility of the proposed workflow across varying spatial resolutions and extents, different sensors (e.g., Landsat and/or Sentinel-2), various vegetation indices (e.g., Enhanced Vegetation Index) and multiple years or periods.

The mapping of the expansion of agricultural use (horizontal intensification) using time-series satellite images yielded satisfactory results given the coarse resolution of the MODIS instruments (250m). The grouping (clustering) of NDVI pixel values showed a similar pattern to that of Global Corine, and this suggests the usability and transferability of the workflow to different areas across the Mediterranean region. Using the same data time-series, we detected the vertical agricultural intensification by implementing an EO-based open-source methodology for the quantification of Rao Q diversity index. The results showed that different patterns of vertical intensification can be detected even across areas with similar crop categories

Agricultural systems are dynamic and there is a growing need for frequent monitoring of agricultural lands in order to assess the extent of horizontal intensification and spatio-temporal diversity and complexity, as they both impact the resilience of farming systems with beneficial and detrimental effects. This report shows that the analysis of relatively dense time series of satellite imagery, such as those provided by the MODIS satellites, can efficiently support the establishment of valuable series of data and enhance the quality of information (in space and in time) towards addressing such issues, especially in relation to capturing elements of agricultural practices intensity, crop rotations, or agro-ecosystem complexity.

Furthermore, our dataset and methodological pipeline should be useful to research scientists and scientist-practitioners working at the interface of spatio-temporal diversity and agricultural systems. Indicators of intensification and landscape complexity in agro-ecosystems are an active field of study, and this deliverable provides a novel, tentative use of Rao's entropy in combination with MODIS EO imagery as a new way to explore them. While the 250m resolution of MODIS products is suitable for regional to national scale analyses and less so for precision farming, it could be informative for large-scale temporal and spatial trends monitoring at relatively low effort. Further work is needed to

discern clearly what elements Rao's entropy captures in farming systems, as well as how the index responds to changes in the scale of computation, since we know that indices of landscape diversity are affected by scale (Merlos and Hijmans2020).

5. REFERENCES

Aramburu Merlos, F., & Hijmans, R. J. (2020). The scale dependency of spatial crop species diversity and its relation to temporal diversity. *Proceedings of the National Academy of Sciences*, *117*(42), 26176-26182.

Bishop, C. M., & Nasrabadi, N. M. (2006). Pattern recognition and machine learning (Vol. 4, No. 4, p. 738). New York: springer.

Bontemps, S., Defournya, P., Van Bogaert, E., Weber, J. L., & Arino, O. (2009). GlobCorine–A joint EEA-ESA project for operational land dynamics monitoring at pan-European scale. In The 33rd International Symposium on Remote Sensing of Environment. Tucson/Arizona USA.

Busetto, L., & Ranghetti, L. (2016). MODIStsp: An R package for automatic preprocessing of MODIS Land Products time series. Computers & geosciences, 97, 40-48.

Defourny, P., Bontemps, S., Bogaert, E., Weber, J., Luis, W., & Soukup, T. (2010). GlobCorine validation report.

Estel, S., Kuemmerle, T., Alcántara, C., Levers, C., Prishchepov, A., & Hostert, P. (2015). Mapping farmland abandonment and recultivation across Europe using MODIS NDVI time series. Remote Sensing of Environment, 163, 312-325.

Golubovic, N., Krintz, C., Wolski, R., Sethuramasamyraja, B., & Liu, B. (2019). A scalable system for executing and scoring K-means clustering techniques and its impact on applications in agriculture. International Journal of Big Data Intelligence, 6(3-4), 163-175.

Lloyd, S. (1982). Least squares quantization in PCM. IEEE transactions on information theory, 28(2), 129-137.

Nguyen, L. H., Robinson, S. V., & Galpern, P. (2022). Effects of landscape complexity on crop productivity: An assessment from space. Agriculture, Ecosystems & Environment, 328, 107849.

Rocchini, D., Marcantonio, M., Da Re, D., Chirici, G., Galluzzi, M., Lenoir, J., ... & Ziv, G. (2019). Time-lapsing biodiversity: An open source method for measuring diversity changes by remote sensing. Remote Sensing of Environment, 231, 111192.

Tsardanidis, I., Bormpoudakis, D., Tsoumas, I., Loka, D. A., Noulas, C., Tsitouras, A., & Kontoes, C. (2025). Estimation of Agricultural Intensification Through Semi-Supervised Deep Learning on Sentinel-2 Imagery. IEEE Journal of Selected Topics in Applied Earth Observations and Remote Sensing.

6. ANNEXES

ANNEX 1. R script for downloading MODIS NDVI time series for each demonstration area.

```
# Set global environment
current_path = rstudioapi::getActiveDocumentContext()$path
setwd(dirname(current_path ))
getwd()

### Install Packages & Get Libraries ----
install.packages(c("MODIStsp","terra","sf","tidyverse","raster"))

library(MODIStsp)
library(terra)
library(sf)
library(tidyverse)
library(raster)

# List MODIS products and available bands
MODIStsp_get_prodnames() # products
MODIStsp_get_prodlayers("M*D13Q1")$bandnames # bands of specific products

# Get bounding box of demonstration area e.g. for the French demonstration area
FR.AOI <- sf::st_read("path_to_file", layer = "FR_AOI") # read shapefile
FR.AOI.rp = st_transform(FR.AOI, 3035) # reproject shapefile
bbox.AOI <- st_bbox(FR.AOI.rp)
bbox.AOI # print bbox

# Download MODIS NDVI series
MODIStsp(gui             = FALSE,
         out_folder      = 'RAW/DZ',
         out_folder_mod  = 'RAW/DZ',
         selprod         = 'Vegetation Indexes_16Days_250m (M*D13Q1)',
         bandsel         = 'NDVI',
         user            = 'xxx', # your username for NASA http server
         password        = 'xxx', # your password for NASA http server
         start_date      = '2022.01.01',
         end_date        = '2022.12.31',
         verbose         = TRUE,
         # bbox for Spanish demonstration region
         bbox            = c (3489240, 1986675, 3718852, 2241935),
         # bbox for French demonstration region
         # bbox            = c (3478307, 2166803, 4137815, 2613471),
         # bbox for Italian demonstration region
         # bbox            = c (4494343, 1386017, 4818458, 1762930),
         # bbox for Algerian demonstration region
         # bbox            = c (3844687, 1408362, 3959185, 1515694),
         # bbox for Egyprian demonstration region
         # bbox            = c (6280379, 1196957, 6293264, 1204900),
         spatmeth        = 'bbox',
         out_format      = 'GTiff',
         compress        = 'LZW',
         out_projsel     = 'User Defined',
         output_proj     = '3035',
         delete_hdf      = TRUE,
         parallel        = TRUE
)
```

ANNEX 2. Terra MODIS and Aqua MODIS NDVI products downloaded and used for Deliverable 2.3

Table 3. Terra MODIS NDVI products downloaded and used for Deliverable 2.3

Satellite data	product	sensor	julianDay	Date
MOD13Q1_NDVI_2022_001	MOD13Q1	Terra	1	01/01/2022
MOD13Q1_NDVI_2022_017	MOD13Q2	Terra	17	17/01/2022
MOD13Q1_NDVI_2022_033	MOD13Q3	Terra	33	02/02/2022
MOD13Q1_NDVI_2022_049	MOD13Q4	Terra	49	18/02/2022
MOD13Q1_NDVI_2022_065	MOD13Q5	Terra	65	06/03/2022
MOD13Q1_NDVI_2022_081	MOD13Q6	Terra	81	22/03/2022
MOD13Q1_NDVI_2022_097	MOD13Q7	Terra	97	07/04/2022
MOD13Q1_NDVI_2022_113	MOD13Q8	Terra	113	23/04/2022
MOD13Q1_NDVI_2022_129	MOD13Q9	Terra	129	09/05/2022
MOD13Q1_NDVI_2022_145	MOD13Q10	Terra	145	25/05/2022
MOD13Q1_NDVI_2022_161	MOD13Q11	Terra	161	10/06/2022
MOD13Q1_NDVI_2022_177	MOD13Q12	Terra	177	26/06/2022
MOD13Q1_NDVI_2022_193	MOD13Q13	Terra	193	12/07/2022
MOD13Q1_NDVI_2022_209	MOD13Q14	Terra	209	28/07/2022
MOD13Q1_NDVI_2022_225	MOD13Q15	Terra	225	13/08/2022
MOD13Q1_NDVI_2022_241	MOD13Q16	Terra	241	29/08/2022
MOD13Q1_NDVI_2022_257	MOD13Q17	Terra	257	14/09/2022
MOD13Q1_NDVI_2022_273	MOD13Q18	Terra	273	30/09/2022
MOD13Q1_NDVI_2022_289	MOD13Q19	Terra	289	16/10/2022
MOD13Q1_NDVI_2022_305	MOD13Q20	Terra	305	01/11/2022
MOD13Q1_NDVI_2022_321	MOD13Q21	Terra	321	17/11/2022
MOD13Q1_NDVI_2022_337	MOD13Q22	Terra	337	03/12/2022
MOD13Q1_NDVI_2022_353	MOD13Q23	Terra	353	19/12/2022

Table 4. Aqua MODIS NDVI products downloaded and used for Deliverable 2.3

Satellite data	product	sensor	julianDay	Date
MYD13Q1_NDVI_2022_009	**MYD13Q1**	**Aqua**	**9**	09/01/2022
MYD13Q1_NDVI_2022_025	**MYD13Q2**	**Aqua**	**25**	25/01/2022
MYD13Q1_NDVI_2022_041	**MYD13Q3**	**Aqua**	**41**	10/02/2022
MYD13Q1_NDVI_2022_057	**MYD13Q4**	**Aqua**	**57**	26/02/2022
MYD13Q1_NDVI_2022_073	**MYD13Q5**	**Aqua**	**73**	14/03/2022
MYD13Q1_NDVI_2022_089	**MYD13Q6**	**Aqua**	**89**	30/03/2022
MYD13Q1_NDVI_2022_105	**MYD13Q7**	**Aqua**	**105**	15/04/2022
MYD13Q1_NDVI_2022_121	**MYD13Q8**	**Aqua**	**121**	01/05/2022
MYD13Q1_NDVI_2022_137	**MYD13Q9**	**Aqua**	**137**	17/05/2022
MYD13Q1_NDVI_2022_153	**MYD13Q10**	**Aqua**	**153**	02/06/2022
MYD13Q1_NDVI_2022_169	**MYD13Q11**	**Aqua**	**169**	18/06/2022
MYD13Q1_NDVI_2022_185	**MYD13Q12**	**Aqua**	**185**	04/07/2022
MYD13Q1_NDVI_2022_201	**MYD13Q13**	**Aqua**	**201**	20/07/2022
MYD13Q1_NDVI_2022_217	**MYD13Q14**	**Aqua**	**217**	05/08/2022
MYD13Q1_NDVI_2022_233	**MYD13Q15**	**Aqua**	**233**	21/08/2022
MYD13Q1_NDVI_2022_249	**MYD13Q16**	**Aqua**	**249**	06/09/2022
MYD13Q1_NDVI_2022_265	**MYD13Q17**	**Aqua**	**265**	22/09/2022
MYD13Q1_NDVI_2022_281	**MYD13Q18**	**Aqua**	**281**	08/10/2022
MYD13Q1_NDVI_2022_297	**MYD13Q19**	**Aqua**	**297**	24/10/2022
MYD13Q1_NDVI_2022_313	**MYD13Q20**	**Aqua**	**313**	09/11/2022
MYD13Q1_NDVI_2022_329	**MYD13Q21**	**Aqua**	**329**	25/11/2022
MYD13Q1_NDVI_2022_345	**MYD13Q22**	**Aqua**	**345**	11/12/2022
MYD13Q1_NDVI_2022_361	**MYD13Q23**	**Aqua**	**361**	27/12/2022